Carbonates and Evaporites (2022) 37:26
https://doi.org/10.1007/s13146-022-00769-2

ORIGINAL ARTICLE

Mixed carbonate-siliciclastic reservoir characterization and hydrocarbon accumulation process of the Ganchaigou area in the western Qaidam Basin, Tibet Plateau

Hai Wu[1] · Hui Liu[2] · Long Wang[3] · Lili Gui[1] · Cheng Yang[4] · Lixin Wang[2]

Accepted: 23 March 2022 / Published online: 25 April 2022

Abstract

The reservoir characteristics and palaeo-fluid evolution process of Ganchaigou area in west Qaidam basin was analyzed through microscopic observation, fluid inclusions, quantitative grain fluorescence and tectonic evolution history. The reservoir rock in the Ganchaigou is dominated by carbonate rock and the pore space. The Ganchaigou area has experienced two stages of hydrocarbon charge and the destruction of late shallow reservoirs: the first stage was the deposition period of the Shangganchaigou Formation (approximately 27 Ma), which experienced low-mature and immature crude oil charge, with a Ro range from 0.35 to 0.72%. It has the characteristics of continuous accumulation of shale oil under self-sealing and self-storage conditions. The corresponding fluid inclusions are mainly yellow–brown and yellow in fluorescence color. The development of saline lacustrine source rocks, the early rapid burial of source rocks and tight carbonate-siliciclastic reservoir made the accumulation of early crude oil possible. The second stage is the late deposition period of the Xiayoushashan Formation (approximately 15 Ma ago), which experienced mature crude oil charge, with a Ro range from 0.51 to1.11%. Affected by the Himalayan orogenic movement, the shallow and deep traps formed a vertical stacking relationship, leading to a deep and shallow multilayered hydrocarbon accumulation model. After the deposition of the Shangyoushashan Formation, orogenic activities in the Eastern Kunlun Range and Altyn Tage Range intensified, a large amount of denudation in the shallow strata occurred, and the integrity of shallow local traps was destroyed, resulting in the loss of crude oil from the shallow traps and a large amount of oil sands forming in outcrop. The traps developed in deep strata still have great exploration potential in this area.

Keywords Qaidam basin · Ganchaigou · Fluid inclusion · Quantitative grain fluorescence · Source rock · Tibet plateau

Introduction

Carbonate and clastic rocks are the two most common types of reservoirs in most oil fields. Bedrock and igneous reservoir may be involved in some oilfields, howerer, the overall proportion is small. In contrast, mixed rock hydrocarbon reservoirs are even rarer. Although mixed rock reservoirs are rare, they have good oil and gas storage performance (Feng et al. 2013; Gao et al. 2018). Mixed sediments were first thought to be sediments formed by mixing terrigenous clastic and carbonate rocks (Mount 1984), and some scholars have made further study about the phenomenon of mixed sediments (Roberts 1987; Doyle and Roberts 1988; Yose and Heller 1989; Dolan 1989). Later, some scholars put forward the concept of mixed rocks (Yang and Sha 1990), and believed that mixed rocks refer to rocks with mixed terrigenous clastic and carbonate components. Siliceous clastic

✉ Hai Wu
wuhai2012@hotmail.com

[1] Research Institute of Petroleum Exploration and Development, PetroChina, Beijing 100083, China

[2] Well Testing Company, Xibu Drilling Engineering Company Limited, CNPC, Karamay 834000, China

[3] Research Institute of Exploration and Development, PetroChina Changqing Oilfield Company, Xi'an 710018, China

[4] Gasfield Development Department, CNPC Qinghai Oilfield Company, Dunhuang 736202, China

rocks and carbonate rocks are not two completely different fields, they belong to a unified whole (Doyle and Roberts 1988). The formation of mixed rocks requires a balance between terrigenous clastic supply and carbonate production (Chiarella et al. 2017).

Mixed rocks complicate deposition, reservoirs, and hydrocarbon migration process, making the analysis of petroleum systems more difficult than conventional reservoirs (Campbell 2005; Palermo et al. 2008; Feng et al. 2011; García-Hidalgo et al. 2007; García-Garcíaet et al. 2009). In saline lacustrine basins and saline foreland compression basins, it often leads to the existence of mixed rocks (Warren 2006). Saline lacustrine basins, due to the rapid changes in the salinity during the geological historical period, resulted in a complicated vertical stacking relationship between the lithology of the lake basin sediments. A complete salinization sequence usually starts with fresh water and gradually progresses to brackish water (Warren 2006; Wang 2018; Wu et al., 2016c). As the lake became salty, deposits changed from clastic rock to carbonate deposits, and finally to salt and other evaporite rocks. The existence of multiple salinization sequences and the frequent fluctuation of the water lead to mixed deposits of multiple lithologies (Warren 2006; Wu et al. 2020). The mixed rock deposited from the salinization sequences environment belongs to primary origin. Give rise to the presence of salt formations in the foreland basins, the formation folds under the compression of tectonic stress, forming mixing lithology in space. The mixed rocks formed from tectonic activity belong to the late transformation origin.

The primary sedimentary mixed rock is mainly controlled by the influence of the saline sedimentary sequence of the lacustrine basin. Due to changes in the salinity of the water, the basin forms multiple salty sedimentary sequences in time and space, and a single salty sequence controls this complete combination of source, reservoir and cap, so rapid water fluctuations will form multiple salty sequences in space, forming multi-layered hydrocarbon accumulation. If strong tectonic movement is experienced in the later stage, the primary mixed rock will be further complicated and the complex reservoir space of fault block and breccia will be formed.

Complex piedmont structural areas often undergo multi-stage tectonic activity and multi-stage of hydrocarbon generation, migration, accumulation and adjustment. Therefore, the hydrocarbon accumulation process and preservation conditions are critical to the forming of current hydrocarbon reservoirs (Wu 2015; 2016a; 2016b). A good configuration between the trap forming and hydrocarbon charge time is conducive to the formation of large oil and gas reservoirs. Fluid inclusions dating technology combined with quantitative grain fluorescence and other ancient reservoir analysis technologies can determine the time of hydrocarbon activity process. Cooperated with the trap evolution and the thermal evolution process of the source rock can further understand the hydrocarbon accumulation evolution and later adjustment process.

The hydrocarbon in Ganchaigou area mainly accumulated in the mixed rock layer of E_3^2 Member. Meanwhile, there are obvious oil seepage on the surface. The reservoirs in this area have obviously undergone later adjustment and transformation, the hydrocarbon accumulation process is not clear. This study combines rock mineral X-ray diffraction (XRD) analysis, thin section, scanning electron microscopy (SEM) and other reservoir analysis methods to carry out the characterization of the mixed rock reservoir in the Ganchaigou area of the Qaidam Basin. With the help of fluid inclusion microscopic observation, homogenization temperature (Th) measurement and basin modeling technologies, the burial history, thermal history, and trap evolution history are unraveled. Moreover, combined with actual geological data, the hydrocarbon evolution process and exploration potential in the Ganchaigou area can be addressed, which is of great significance to the petroleum exploration and deepening geological understanding in the basin.

Geological setting

The Qaidam Basin is one of the main petroliferous basins formed during the uplift of the Tibet Plateau (Harrison et al. 1992; Chung et al. 1998; Zhisheng et al. 2001; Wang et al. 2008; Yu et al. 2019). Due to the collision between the Asia-Europe plate and the Indian plate, the Tibet Plateau continued to uplift and push northward, and the crust slipped northward and eastward to escape, forming large-scale strike-slip and thrust faults, resulting in the uplift of ranges and flexural basins (Harrison et al. 1992). According to the distribution and characteristics of the main petroleum exploration areas, the basin is divided into five first-order tectonic units, namely the western Qaidam depression zone, the Altyn Tage Range (ATR) front zone, the Qilian Range front zone, the eastern Qaidam Sanhu depression zone, and the abdominal anticline zone. The study area in this paper is located in the western Qaidam depression. A large Cenozoic petroleum system develops in the western Qaidam area. Its main source rock is the upper member of Xiaganchaigou Formation (E_3^2) of the Paleogene (Zhang et al. 2017a). The main hydrocarbon reservoirs span multiple strata, from the Paleogene to the Neogene. The hydrocarbon-bearing characteristics of this multilayered system are not only related to the multi-phase tectonic movement, but also to the large-scale mixed rock reservoir formed under the control of the multi-phase salinization sequence in the area. In the western Qaidam basin, there are multiple saline sedimentary sequences in the E_3^2 Member of the Paleogene (Guo et al.

2019), and there are multiple hydrocarbon-bearing layers in the vertical space. At the same time, under the influence of the piedmont compression structure, the reservoir is further complicated by faults and compression and other tectonic effects, forming multi-fault blocks and multi-layer oil and gas accumulations. With the deepening exploration in the western Qaidam basin, the focus of exploration targets gradually shifted to the deep Paleogene. The mixed rocks are dominated by carbonate, and some sections develop clastic rocks. Generally speaking, the lithology of the reservoir is relatively tight, mainly relying on carbonate intercrystalline pores, dissolved cavities and fractures as the main storage space (Liu et al. 2021). A good salt caprock layer is also developed on the top of this interval, which can form a good deep source-reservoir-seal combination in E_3^2 Member.

With the large-scale oil and gas discoveries in the Yingxiongling area in western Qaidam basin, especially the breakthrough in the deep layers of Yingxi, petroleum exploration in the Yingxiongling area has become a hot spot. The Ganchaigou area is adjacent to the northern part of the Yingxiongling area in western Qaidam basin (Fig. 1), with the Xianshuiquan area in the northeast and ATR in the northwest. The northeast-southwest trend is generally represented as a fault anticline structure, and the northwest-southeast trend is a large nose structure. The fault slipped inside the E_3^2 Member, and the strata overlapped and repeated vertically in the shallow Ganchaigou area. Affected by the Himalayan orogeny, the ATR and the EKR formed strike-slip uplift structures, which had a key influence on the formation and later transformation of the main petroliferous structures in the western Qaidam Basin. The formation of the structure in the western Qaidam area is similar to that in the Yingxi area. The embryonic structure was formed relatively early (Guan et al. 2017; Wu et al. 2021a). In the later period, the trap uplift was further aggravated by the compression and uplift orogeny, and the closure height and area were enlarged. The stratum uplift is obvious in the late period, which has an obvious reforming or destructive effect on the structure formed in the early period.

The main source rocks in the Ganchaigou area are similar to those in the Yingxi area, and they are both fine-grained mixed rocks of the upper member of the Xiaganchaigou Formation. The main reservoirs are the carbonate rock and a small amount of argillaceous siltstone, sandy limestone, sandy mudstone and gypsum mudstone in the upper member of the Xiaganchaigou Formation. The Shangganchaigou Formation and Xiayoushashan Formation in the shallow part are also well-developed reservoirs, but in the late period due to the rapid uplift of ATR and EKR (Meyer 1998; Jolivet et al. 2003; Fu 2007; Yin 2007; 2008a; 2008b; Zhang 2012; Cheng 2014), causing the integrity of the shallow strata caprock to be locally damaged by the fault, so the shallow preservation conditions are relatively poor.

Materials and methods

Sampling

The mixed rock reservoirs have become the main areas for oil production in the western Qaidam basin. Some wells with daily output of 1,000 tons of oil equivalent have been

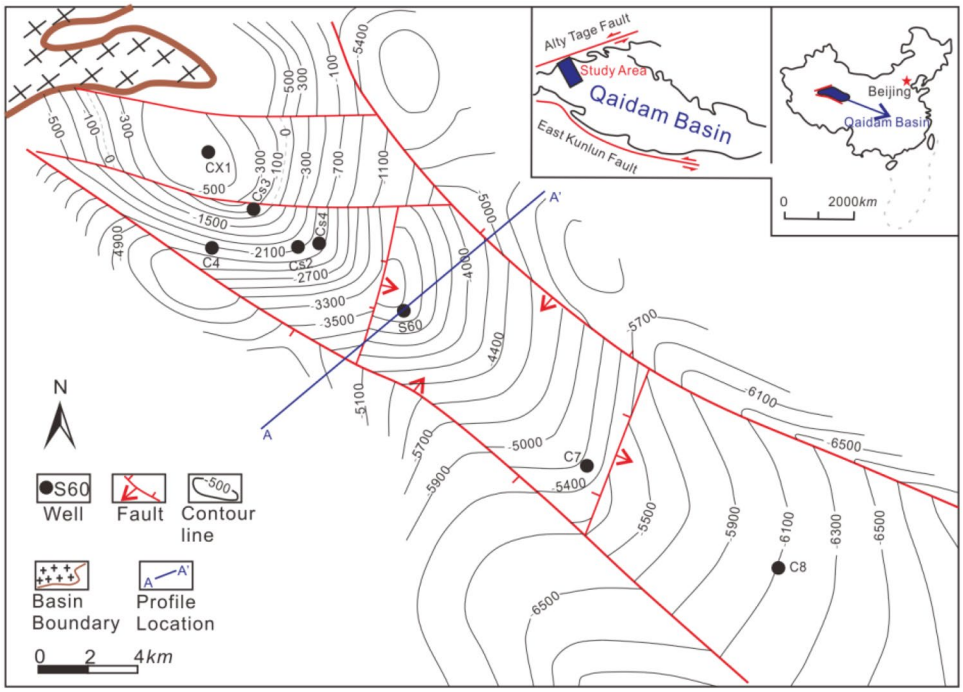

Fig. 1 Plane structure map of the upper member of Xiaganchaigou Formation (E_3^2) in the Ganchaigou area, Qaidam basin

discovered in this area, which have made significant contributions to the increase of oil reserves and production in the Qaidam basin, and also promoted the surrounding areas petroleum exploration.

Twenty-nine core samples from five wells (CX1, S60, S3-1, X102 and X10) were collected for the integrated petrologic and geochemical study. All samples were obtained from the main oil-bearing layer Xiaganchaigou Fm. (E_3^2). The mixed lithologies of the selected samples were dominated by carbonate rock, followed by clastic rock. The preprocessing steps for quantitative fluorescence technique (QFT) analysis samples can refer to (Liu and Eadington 2005).

X-ray diffraction (XRD)

Ten core samples were selected from well S60 to make the XRD analysis by using an Empyrean made by Netherland. The maximum power of the instrument can be up to 2.2 kW, and the maximum counting rate is more than 109cps, and the sample can be corrected in five directions at the same time. The ten samples are all from the mixed rock of E_3^2 of the Ganchaigou area in the western Qaidam basin.

Petrography

The microscope used for optical observation was carried out on thin section by using a Zeiss Axiom Imager M2 with a magnification of × 1000 under incident-light, reflected-light, and ultraviolet-light (UV) modes. The UV micro-fluorescence observations were made by using Zeiss Axiom Imager M2 optical microscope equipped with an HBO-100 epi-fluorescence source filtered at 365 ± 5 nm and an LP400nm emission filter. The cement phase, fractures, veins, cross-cutting relationship of fluid inclusions were recognized by using the optical and fluorescence. Mineral identification and pore type observation were mainly observed by single polarized light and orthogonal light mode.

Quantitative fluorescence techniques (QFT)

Three fluorescence techniques, quantitative grain fluorescence (QGF), quantitative grain fluorescence on Extract (QGF-E) and total scanning fluorescence (TSF), can detect palaeo-oil zones and current residual oil zones in petroleum wells (Liu and Eadington 2005; Liu et al. 2014). QGF can be used to characterize palaeo-oil reservoirs by detecting the hydrocarbon information inside the mineral particles. The QGF-E can identify the characteristics of current oil reservoirs by detecting the components of hydrocarbons adsorbed on the surface of mineral particles. Meanwhile, it can be used to compare with palaeo-oil reservoirs to study the evolution process of oil and gas reservoirs (Liu and Eadington 2005). The QGF index is the ratio of the QGF intensity to the fluorescence intensity corresponding to the wavelength of 300 nm. The higher the QGF index, the better the oil-bearing properties of the palaeo-reservoir will be (Liu and Eadington 2005; Liu et al. 2007). The QGF-E intensity can be used to intuitively judge the current oil-bearing strength of the reservoir.

TSF can be used to identify information such as the composition and maturity of crude oil or adsorbed hydrocarbons in the reservoir. It also can be used as a tool for oil source comparison and petroleum migration pathway identification (Liu 2007). R_1 is an important indicator in TSF technique indicating that the sample is excited by a 270 nm laser, corresponding to the ratio of the fluorescence intensity of the emission wavelength of 320–360 nm, which is similar to the ratio of tricyclic aromatic hydrocarbons and monocyclic aromatic hydrocarbons in crude oil (Liu 2007). R_1 can be used to characterize the maturity of adsorbed hydrocarbon or crude oil. It is generally considered that when $R_1 < 2.0$ is condensate to very light oil, when $2.0 < R_1 < 3.0$ is light-normal oil, and when $R_1 > 3.0$ is medium-heavy oil.

Microthermometry of fluid inclusions

Homogenization temperature (Th) measurements were obtained using a microscope-mounted Linkam Thms-Q 600 heating-freezing stage. The heating rate were set to 5–10 °C/min at the beginning, changed the heating rate to 0.5–1 °C/min when the inclusions are close to uniform. The precision of Th measurements was about 1 °C.

Basin modeling

The burial history and thermal evolution history of the Ganchaigou petroleum system were modeled using the PetroMod 1D software. The drilling data from the drilling report of PetroChina and the published boundary conditions (Li et al. 2015) were used to carry out the modeling. The bottom hole temperature and vitrinite reflectance data were used to calibrate and validate the thermal history result of the model.

Results

Reservoir characteristics

Mineral composition

The lithology of this mixed rock reservoir is mainly carbonate rock, followed by clastic rock. Through X-ray diffraction (XRD) analysis of the lithologic minerals of the E_3^2 Member in well S60, the results show that the composition of this mixed rock reservoir is mainly dolomite and calcite. Among

the carbonate rock components, calcite and ankerite account for the highest proportion. For example, the carbonate mineral content accounts for more than 74% and the ankerite accounts for 60.7% in the depth of 3032.93 m. The content of clastic rocks in a few intervals is also high, for instance, the mineral content of clastic rocks at a depth of 3034.35 m accounts for more than 58% (Fig. 2).

Pore characteristics

Give rise to the development of multiple lithologies and multi-phase tectonic movements, various types of reservoir spaces develop in the Ganchaigou area. Among them, it is divided into primary and secondary storage space, and the later secondary storage space is dominant. The primary reservoir space mainly includes residual pores, intercrystalline pores and deposit genesis bedding fractures (Fig. 3). The residual pores filled with dolomite particles are relatively large, and the larger residual pores observed in the microscope can reach 4 mm (Fig. 3a), but this type of pore is relatively rare. The size of intercrystalline pores in dolomite is relatively small (Fig. 3b), making it difficult to become a major crude oil storage space. The bedding fractures of sedimentary origin mostly appear in the mixed rock development area, especially in the sandy limestone development area. The seepage capacity and storage capacity of the reservoir can be greatly improved for the existence of bedding fractures, but this kind of reservoir does not occupy the mainstream in Ganchaigou area.

The secondary reservoir space in Ganchaigou area is relatively developed, mainly including dissolution pores and fractures. The dissolution pores are mainly distributed in dolomite and limestone (Fig. 3d, f, g). Some dissolution pores are developed in the gypsum grains (Fig. 3e), while some dissolution pores are developed in the mixed area of sandy limestone. A large number of pores are formed by dissolution, and some quartz particles and marl content remain after dissolution (Fig. 3g, h, i). Due to the occurrence of multi-episode tectonic movement in the geological history in Ganchaigou area, a large number of fractures were formed in the reservoir. Give rise to the salty sedimentary environment of the western Qaidam basin, the fractures were mostly filled by carbonate and evaporate. The secondary dissolution pores mostly developed along the structural fractures (Fig. 3d, g), forming a large number of dissolution fracture-cavity networks reservoir system.

Dissolution pores are well developed in some intervals in the Ganchaigou area, but the connectivity of the pores is poor. High-angle fractures develop in some interval, however, due to the low fracture density and number, the fracture connectivity rate is low. By measuring the porosity and permeability of reservoir core samples, the results indicate that the average porosity of 84 samples was 7.57%, and porosity below 8% accounted for 83% (Fig. 4). The overall reservoir is tight and the pores are poorly developed. The average permeability of the 58 samples is 0.58md, and samples permeability at 0.1md accounted for 84%. The reservoir permeability is also low. Generally speaking, the reservoirs in this area have the characteristics of low porosity and low permeability (Fig. 4). Low porosity and low permeability are typical characteristics of general carbonate samples (Rashid et al. 2015, 2017), but the development of dissolution pores or fractures in some samples will greatly increase the porosity and permeability of the reservoir. Since the upper member of the Lower Ganchaigou Formation is a self-generating and self-storing oil reservoir, its hydrocarbon supply conditions will not become a problem that restricts petroleum

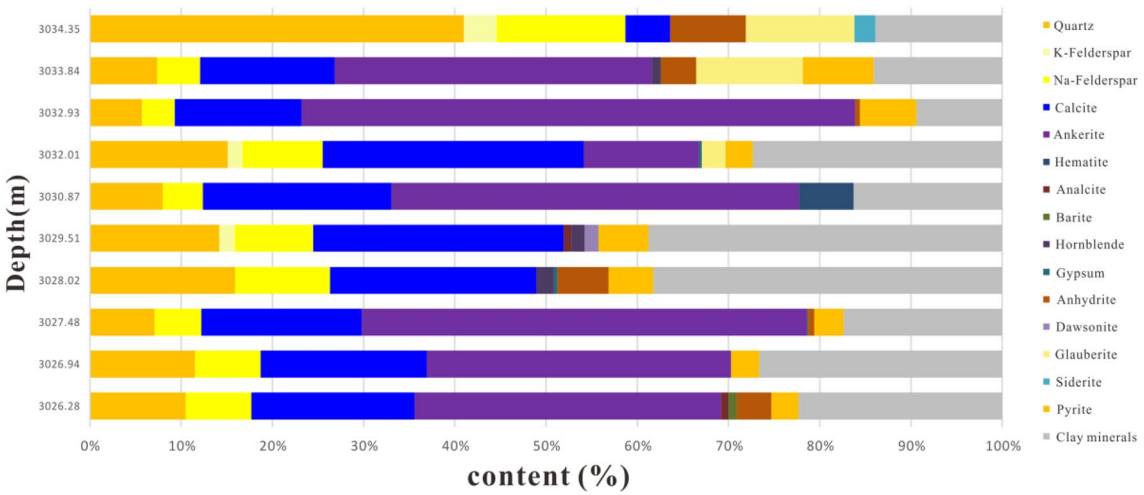

Fig. 2 Mineral composition of the upper member of the Xiaganchaigou Formation (E_3^2) in the Well Shi 60

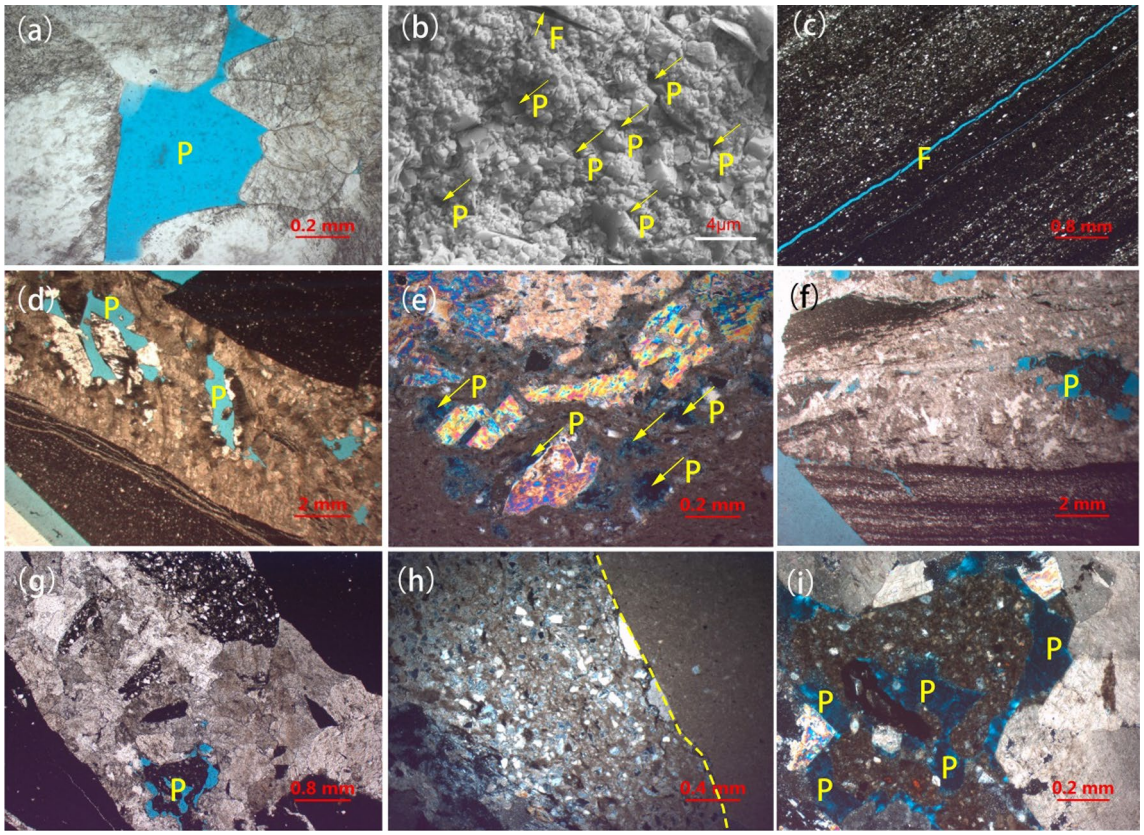

Fig. 3 Microscopic characteristics of the pore space of the mixed rock reservoir in the Ganchaigou area. **a** Well S60, dolomite residual intergranular pores, 3447.76m, E32, **b** Well S60, carbonate intercrystalline pores, 3027.17m, **c** Well S60, micrite limestone bedding fractures, 3454.61 m, **d** Well S60, dissolution pores inside calcite veins, **e** Well S60, gypsum limestone, dissolution pores of gypsum particles, 3335.5m, **f** Well Shi60, sandy marl, in mixed rocks Dissolution holes in anhydrite, 3372.5m, **g** S60 well, sandy limestone, internal dissolution holes in the mixed zone of clastic rock and carbonate rock, 3566m, **h** S60 well, sandy limestone, clastic Dissolution holes in the mixed zone of rock and carbonate rock, 3566m, **i** Well S60, sandy limestone, dissolution holes in the mixed zone of clastic rock and carbonate rock, 3566m. The blue color in the photographs represents the pore space. The arrows in the Figures indicate pores. *P* pore, *F* fracture

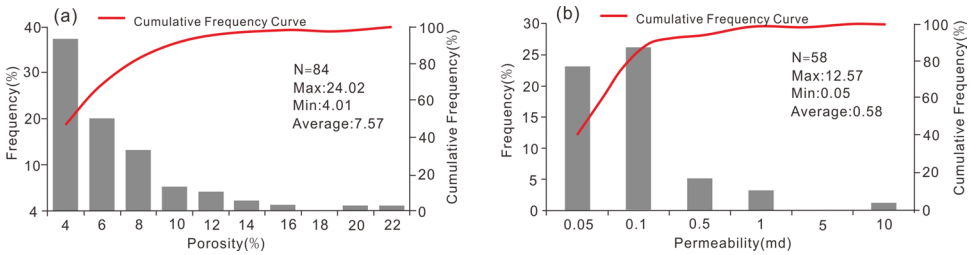

Fig. 4 Reservoir physical properties of the upper member of the Xiaganchaigou Formation (E_3^2) in the Ganchaigou area

accumulation. This type of oil reservoir will mostly undergo artificial volume fracturing to increase productivity.

QFT characteristics

The characteristics of QGF and QGF-E

The Paleogene reservoirs in the Ganchaigou area are generally tight, and the reservoirs are mostly stratified or discontinuous, and there is no uniform oil–water interface. The palaeo-reservoirs and the current ones mostly have the characteristics of inheritance or late transformation.

The QGF index of the core sample of well S60 in the vicinity of Ganchaigou is not much different from the value of the adjacent well X10, which basically fluctuates around 4 to 5 (Table 1), indicating that some hydrocarbon charge occurred in the early period. However, from the perspective of the QGF-E intensity (Table 1), the S60 well block is generally above 20 pc, while the X10 well block is generally low, indicating that hydrocarbon is well preserved in the

Table 1 Quantitative fluorescence data table of reservoirs in Ganchaigou area

Sample no	Depth/m	Layer	QGF		QGF-E		TSF			R_1
			QGF index	λmax/nm	QGF-E intensity	λmax/nm	TSF max/pc	Max Ex/nm	Max Em/nm	
S60_1	3034.24	E_3^2xg	5.53	403	21.03	378	17.11	256	386	3.76
S60_2	3034.34	E_3^2xg	5.25	393	29.03	374	24.0	258	373	3.76
S60_3	3034.84	E_3^2xg	5.85	400	36.20	377	30.1	256	376	3.59
X10_1	1071.6	E_3^2xg	3.98	401	21.28	374	17.6	256	371	4.08
X10_2	2336.47	E_{1+2}	4.73	394	0.77	366	4.2	220	420	1.00
X10_3	2336.47	E_{1+2}	5.37	391	0.86	367	4.6	220	405	1.51
X10_5	2338.97	E_{1+2}	4.51	393	0.91	360	3.3	220	265	1.28
X10_6	2344.6	E_{1+2}	5.38	393	0.82	355	4.8	220	420	1.56
CX1_5	4600.7	J_{1+2}	5.60	393	7.35	373	11.5	220	420	2.94
CX1_9	4601.6	J_{1+2}	5.34	395	1.65	370	8.3	220	420	2.30
CX1_10	4601.7	J_{1+2}	4.32	396	2.03	374	11.3	220	415	2.00
X102	2062.2	E_3^2xg	4.40	399	9.79	375	11.3	220	420	3.09

E_3^2 formation of S60 well block, while the X10 well block obviously experienced leakage in the late period. The fluorescence spectrum peak (λmax) of QGF or QGF-E can be used to characterize the maturity information of crude oil. From λmax values of QGF and QGF-E spectra in Ganchaigou area (Table 1, Fig. 5), the range of QGF is 391 ~ 403 nm, and QGF-E is 355 ~ 378 nm, which is significantly smaller than the λmax of QGF spectra. It shows that the current reservoir is filled with relatively high-mature hydrocarbon in the late episode and mixed with early hydrocarbon, showing relatively high maturity characteristics.

Characteristics of TSF

TSF can be used to identify information such as the composition and maturity of crude oil or adsorbed hydrocarbons in the reservoir, and can be used as a tool for oil source comparison and crude oil migration pathway identification (Liu 2007). R_1 can be used to characterize the maturity and composition information of crude oil or hydrocarbons inside inclusions. The R_1 of S60 well block is between 3.59 and 3.76%, which is the characteristic of medium oil. The overall R_1 of the X10 well area, ranging from 1.0 to 1.56%, is lower than that of the S60 well area. Some shallow layer samples such as 1071.6 m appear abnormally high R_1 value (Fig. 6) shows the presence of heavy components (mainly residual bitumen), reflecting the late shallow oil reservoir destruction. The TSF spectra of the reservoirs in the Ganchaigou area and adjacent areas all show a single peak, indicating that the hydrocarbon in the current reservoir is from the same source rock. Give rise to the burial depth, it may experience destruction in the shallow strata, and continuously accumulated early low-mature and late-stage relatively mature oil in deep strata where preservation conditions are relatively good.

Hydrocarbon charge period and accumulation process

Petrography of fluid inclusions

The main reservoir in the Ganchaigou area is located in the E_3^2 Member mixed rock, and inclusions are mainly developed in calcite veins and quartz healing fractures. It is difficult to find inclusions in the host carbonate rocks of primary deposition, and only the fluid inclusions captured in the process of burial and diagenesis can record the time and characteristics of fluid charge. Fluid inclusion petrography usually uses information such as the occurrence relationship of inclusions in mineral particles, the single polarized color and the fluorescence color of the inclusions, the fluid phase state, and the gas–liquid ratio to classify and stage the development of inclusions (Munz

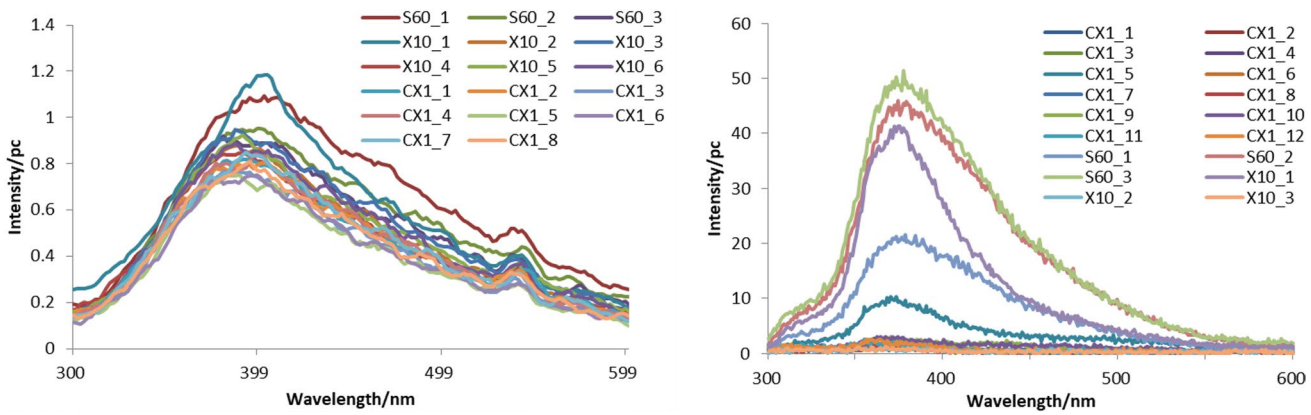

Fig. 5 QGF (**a**) and QGF-E (**b**) spectra of reservoirs in Ganchaigou area, western Qaidam Basin

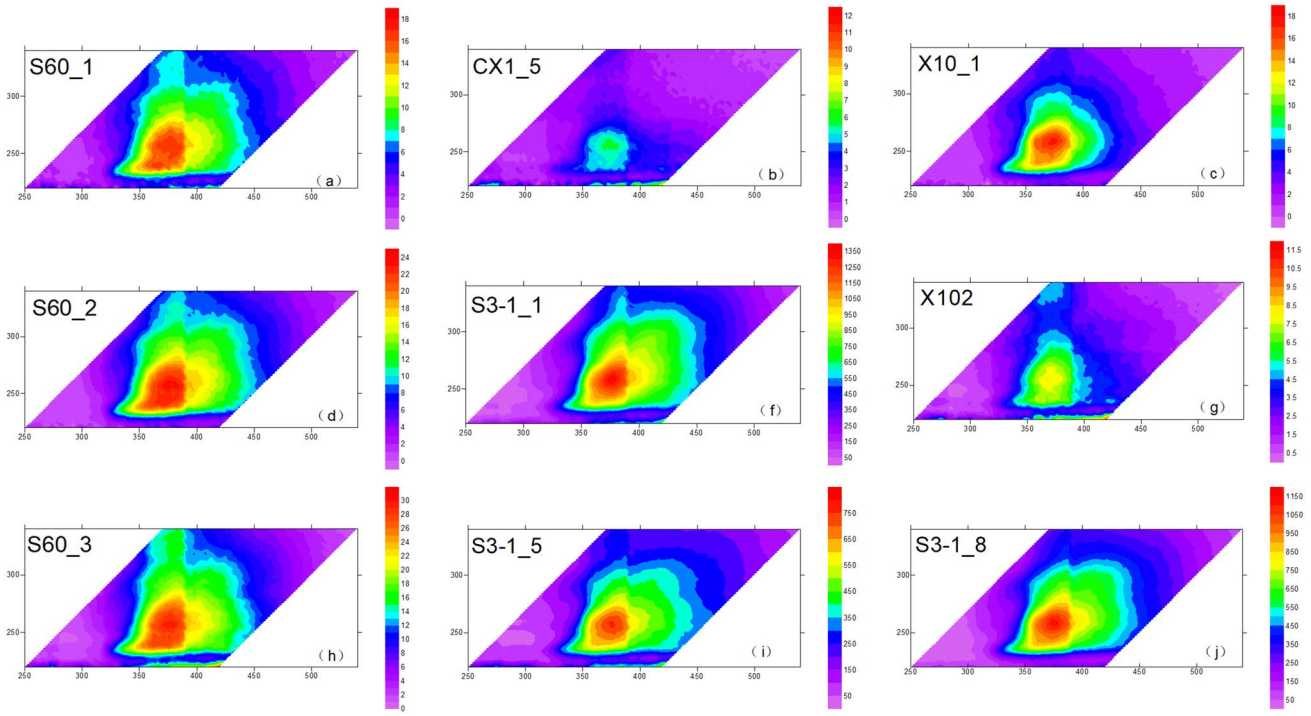

Fig. 6 Total scanning fluorescence (TSF) spectrum characteristics of Ganchaigou and adjacent areas

2001; Goldstein 2001; Wu et al. 2015, 2016a, 2016b, 2016c). Some scholars also use the fluorescent color of hydrocarbons fluid inclusions to classify the phases, which is a way to quickly identify the time when hydrocarbons formed. With the increase of hydrocarbon maturity, the fluorescence color of inclusions gradually changes from brown to dark yellow to orange, yellow white to green, blue-green to blue and white (Zhao and Chen 2008; Ping et al. 2017, 2019). This fluorescent color is determined by the carbon chain length of hydrocarbons and the characteristics of branch chain development. The longer the carbon chain, the lower the maturity of the hydrocarbon, which emits yellowish fluorescence. High-mature hydrocarbons have relatively short carbon chains, and their groups emit bluish and white fluorescence under fluorescent irradiation. Because the fluorescence recognition method is a qualitative method of identifying the stage and relative maturity, its application is relatively limited. In addition, due to some fluid inclusions have local micro-ruptures or carbon chain of hydrocarbon ruptures during the burial process, it will lead to the conversion of darker fluorescence to brighter fluorescence in the early stage, which will mislead the formation of successive stages (Wu et al. 2016b). Therefore, in the actual application process, it

is not accurate enough to judge the formation episodes and period only based on the fluorescence color of hydrocarbon fluid inclusions. It is usually combined with the petrography, homogenization temperature of the hydrocarbon inclusions and the associated brine inclusions to make the results more credible. It can be classified into three types according to the occurrence characteristics of fluid inclusions in well S60 of Ganchaigou area.

The first type, developed in the calcite veins with a ring shape, is the yellowish-brown or yellow pure liquid or vapor–liquid two phase hydrocarbon inclusions (Fig. 7a, b, c), and show black or brown color under single polarized light. Most inclusions of this type are pure liquid phases, some of which are vapor–liquid two phase, and the vapor–liquid ratio is low, with a range of 4.1 ~ 17.5%. According to the low vapor–liquid ratio and the yellow–brown fluorescence color of the fluid inclusions, it can be inferred that the hydrocarbons in the inclusions formed at an early period.

The second type, also developed in the calcite veins with nebula or ring shape, is the blue-green or blue pure liquid or vapor–liquid two phase hydrocarbon inclusions (Fig. 7d, e, f), and present brown color under single polarized light. In another case, the calcite veins of this type of inclusions cut by linear healing seams show blue and blue-green fluorescence, and they also show dark brown color under single polarized light. Moreover, most of this type of hydrocarbon inclusions presents pure liquid phase, while a small

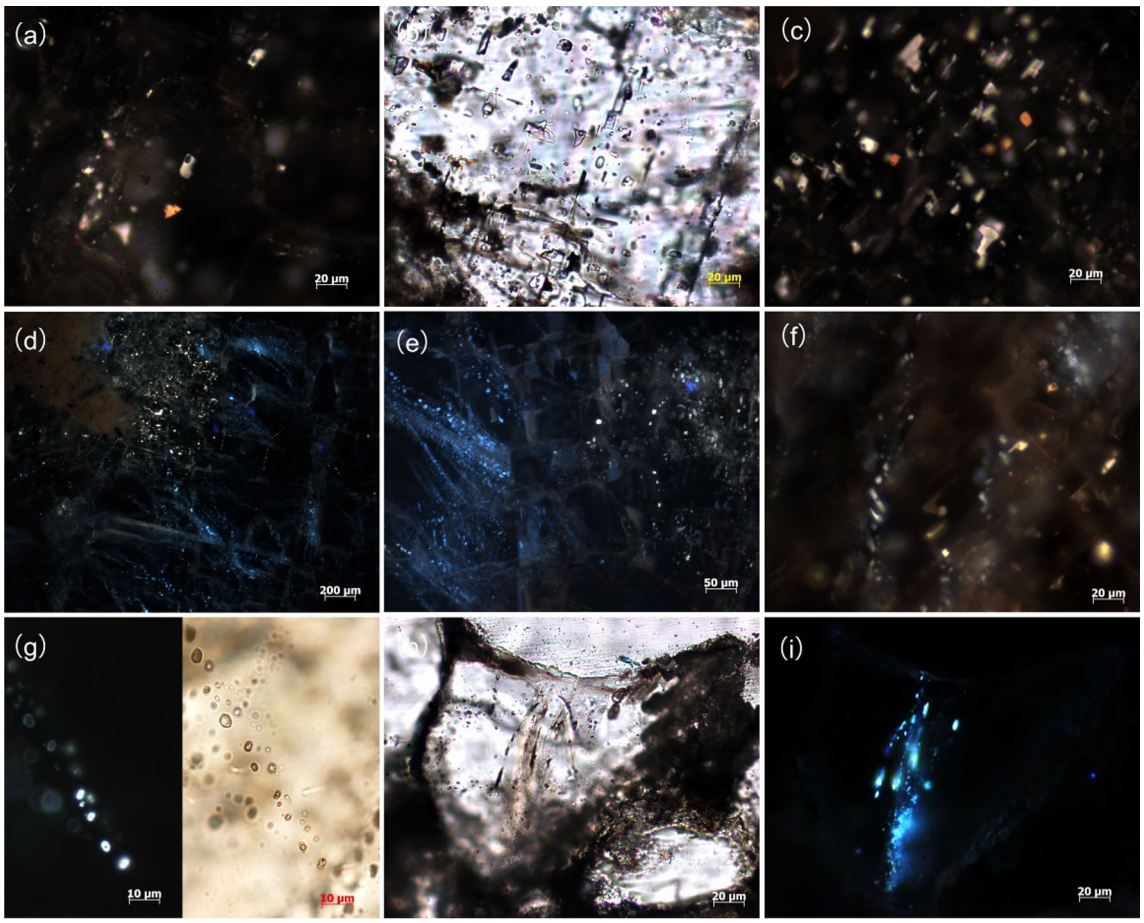

Fig. 7 Petrographic characteristics of fluid inclusions in Ganchaigou area, Qaidam Basin **A** yellow and yellowish brown fluorescent hydrocarbon inclusions in calcite vein, 3338.65 m, E_3^2, UV in well S60, **B** hydrocarbon inclusions in calcite vein in well S60, 3338.65 m, E_3^2, single polarized light, **C**: yellow and yellow brown fluorescent hydrocarbon inclusions in calcite vein in well S60, 3338.65 m, E_3^2, UV, **D** Well S60, calcite vein internal yellow and yellow brown fluorescent hydrocarbon inclusions, 3338.65 m, E_3^2, UV, **D** Well S60, calcite vein internal hydrocarbon inclusions, 3338.65 m, E_3^2, UV In well shi-60, the yellow green fluorescent hydrocarbon inclusions and blue fluorescent hydrocarbon inclusions in calcite veins are distributed linearly, 3338.65 m, E_3^2, UV, **E** 1 In well S60, the yellow white fluorescent hydrocarbon inclusions and blue fluorescence in calcite veins are linearly distributed, 3338.65 m, E_3^2, UV, **F** yellow white fluorescent hydrocarbon inclusions in calcite veins in well S60, 3338.65 m, E_3^2, UV, **G** in well S60, the blue and white fluorescent hydrocarbon inclusions in the quartz grain healing fracture are linear distribution, 3034.84 m, E_3^2, left UV + right single polarized light, **H** in well S60, the distribution of hydrocarbon inclusions in the fracture of quartz particles is linear, 3034.84 m, E_3^2, single polaried light; in well S60, the distribution of blue fluorescent hydrocarbon inclusions is linear, 3034.84 m, E_3^2, UV)

amount present vapor–liquid two phase, with relatively low vapor–liquid ratio. They are usually associated with the first type of yellow and yellowish-brown fluorescent hydrocarbon inclusions in calcite veins.

The third type is hydrocarbon inclusions in the healing fractures of quartz grains developed in a mixed rock reservoir (Fig. 7g, h, i), which usually show linearly distribution cutting through quartz grains. This type of fluid inclusions is mostly blue fluorescence, and present yellow–brown color under single polarized light, with a higher vapor–liquid ratio around 17.4 ~ 23.5%.

Hydrocarbon charge period

The theoretical premise for the study of the uniform temperature of fluid inclusions is that the volume of fluid inclusions remains unchanged during the burial process after formation and is captured under uniform phase conditions (Munz 2001; Goldstein 2001). In fact, there will be a certain difference in the homogenization temperature of hydrocarbon inclusions and associated brine inclusions captured during the same period. It is generally believed that the associated brine inclusions can better reflect the geological conditions during the capture period. This is because hydrocarbon inclusions may have certain changes during the later burial process.

The fluid inclusions developed in the core samples of well S60 are mainly hydrocarbon inclusions, and the number of associated brine inclusions is relatively small. The Th range of yellow–brown and yellow fluorescent oil inclusions is mainly concentrated around 55 ~ 85 °C (Fig. 8), and the associated brine inclusions are less developed. The small amount of associated brine inclusions Th is mainly around 71 ~ 75 °C (Fig. 8). The Th of blue-green fluorescent and blue fluorescent hydrocarbon inclusions is mainly concentrated between 66 ℃ and 85 ℃, and its Th is slightly higher than that of yellow–brown hydrocarbon inclusions. However, the Th range of yellow–brown hydrocarbon inclusions is larger, and partly coincides with the Th of such blue-green hydrocarbon inclusions, indicating that the charge time of the two hydrocarbons is not much different. It is the product of continuous hydrocarbon charge. Therefore, it can be considered that the two types of inclusions recorded the same period of hydrocarbon charge. Based on the Th data of the brine inclusions associated with the yellow–brown and yellow fluorescent oil inclusions, combined with the burial history and thermal history data (Fig. 9), it can be determined that the crude oil charge time of this period is about 27 Ma, which is the Xiaganchaigou Formation sedimentary period in the Oligocene. The Th of blue and blue-white fluorescent hydrocarbon inclusions is mainly distributed in 100 ~ 120 °C, with a peak value of 110 °C ~ 115 °C (Fig. 8). Combining the history of burial and thermal evolution, it is determined that the crude oil charge time is about 15 Ma (Fig. 9), which is the deposition period of the Xiayoushashan Formation (N_2^1) in the Pliocene.

Configuration between charge time and thermal history

The degree of thermal evolution of source rock is closely related to formation temperature and geological time, and the change of geothermal temperature in unit geological time is closely related to formation burial velocity, that is, for a specific study area, burial history plays a key role in the thermal evolution process of source rock (Gussow 1954; Baur et al. 2018; Wu et al. 2021a, 2021b). In the western of Qaidam Basin, the depocenter changes frequently during the geological historical period, and since the Cenozoic, there has been a trend of migration from southwest to northeast (Meng et al. 2008; Cheng et al. 2018a, b, 2019; Wu et al. 2021a, 2021b). The burial process of strata in Ganchaigou area is more similar to that in southwest Qaidam Basin. Therefore, since the formation of source rocks in the upper

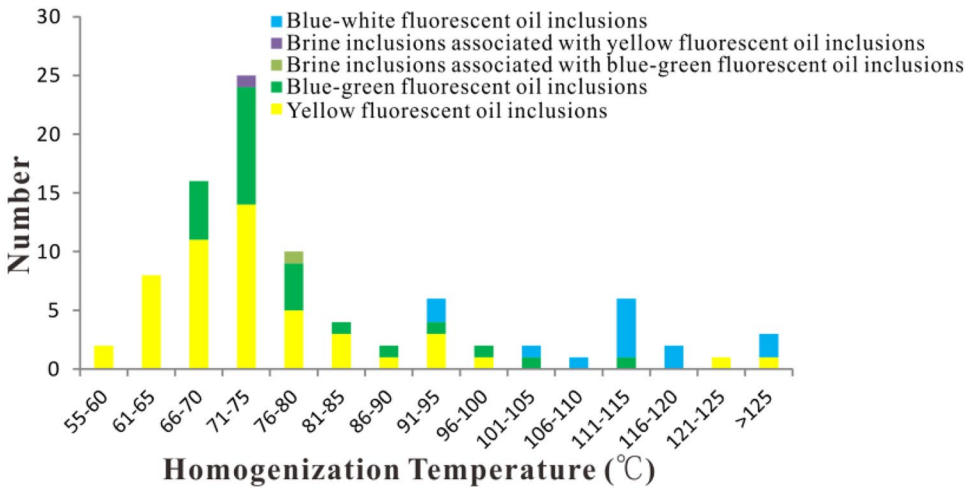

Fig. 8 Homogenization temperature of well S60 in Ganchaigou area

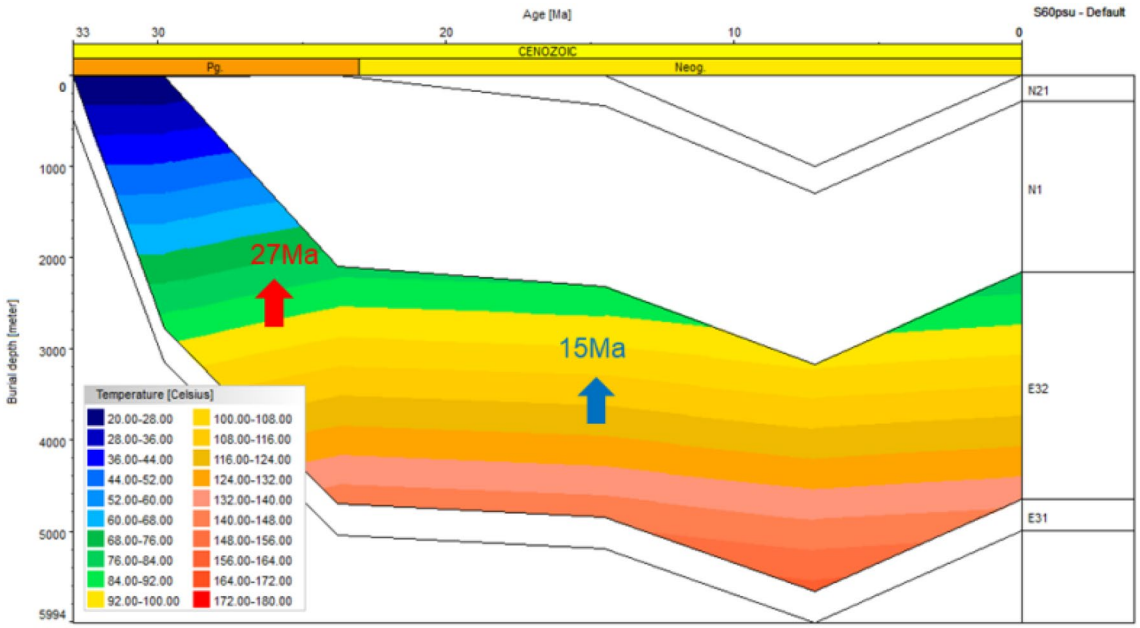

Fig. 9 Burial history and thermal evolution history of well S60 in Ganchaigou area

member of Xiaganchaigou Formation (E_3^2), the burial rate of early Oligocene is relatively fast, and the deposition thickness is large. The burial rate of Pliocene strata is relatively slow and the deposition thickness is thinner. Such "early fast late slow" burial process also makes the thermal evolution process of source rocks present the characteristics of "early fast late slow".

According to the fluid inclusion characteristics, Th data and thermal history, Ganchaigou area experienced two episodes of hydrocarbon charge: the first stage was about 27 Ma, and the second stage was about 15 Ma. According to the thermal evolution diagram of the source rock of well S60 in Ganchaigou area (Fig. 10), the vitrinite reflectance (Ro) of the source rock at the bottom interface of the E_3^2 was 0.72%,

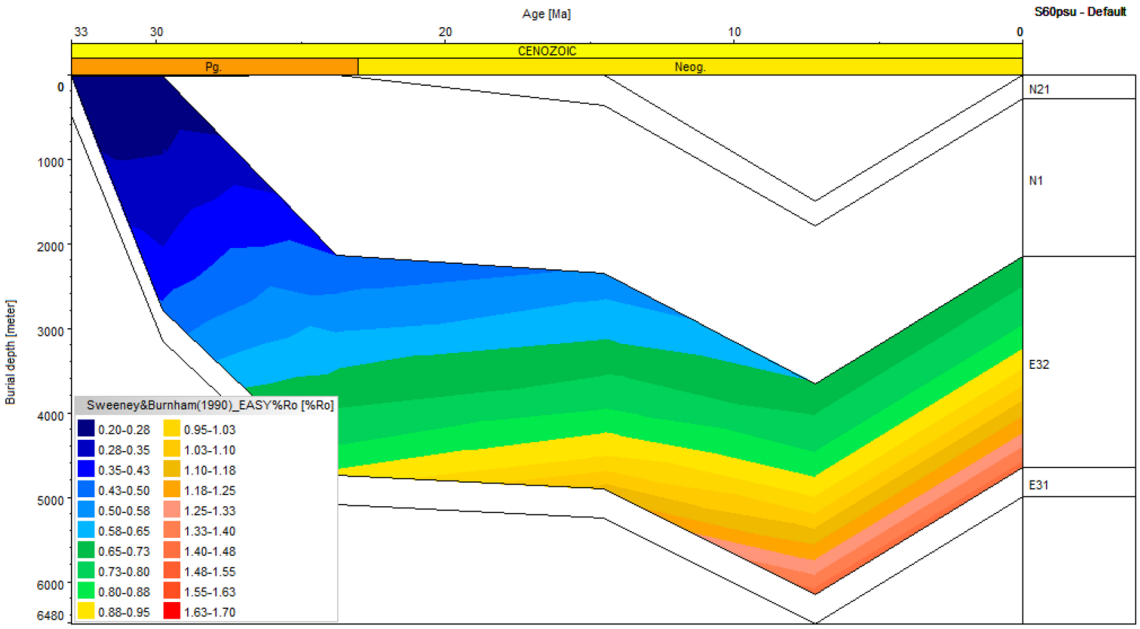

Fig. 10 Thermal evolution history of source rock in Well S60 in Ganchaigou area

while the top interface was 0.35%. In this period, the maturity of source rocks is so limited that it is difficult to generate oil on a large scale. Only the lower part of the E_3^2 Member reaches the stage of generating low mature oil, while the upper layer is still in the immature stage. However, in terms of the abundance of fluid inclusions, the scale of crude oil generated in this period may be relatively large. Subject to the control of the reservoir of E_3^2 Member, the hydrocarbon accumulation is likely to be in a self-generation, self-storage and self-sealed mode. The E_3^2 Member is a low-porosity and low-permeability mixed rock interval, and tectonic is relatively stable in the the first hydrocarbon charge period (~ 27 Ma), the oil generated in the early stage may not be well migrated away from the source rock and stay in the mixed rock reservoir, forming large-scale in-situ accumulation of crude oil and oil inclusions. Some scholars (Liu et al. 2021; Gong et al. 2019, 2021) believe that the crude oil accumulated in this interval belongs to the type of shale oil.

At 15 Ma, the vitrinite reflectivity of the source rock at the bottom interface in the E_3^2 Member was about 1.11%, and the top interface was 0.51%. At this time, the main source rock of E_3^2 Member has generally reached matured and has the ability to generate mature and normal oil. During the deposition period of the Shangyoushashan Formation (N_2^2), affected by the strike-slip and uplift of the ATR and the EKR, the Ganchaigou area gradually began to uplift and some formations were eroded, which has a certain destructive effect on the shallow reservoir.

Discussion

According to the deposition thickness data of the Qaidam basin, the sedimentary center of the Qaidam basin generally has the characteristics of historical migration from west to east, and the depocenter of the western Qaidam basin generally has the characteristics of migration from the southwest to the northeast of the Qaidam basin (Meng et al. 2008; Cheng et al. 2018a, b, 2019; Wu et al. 2021a). Therefore, during the Paleogene period, the thickness of the stratigraphic deposits in the area near the ATR in western Qaidam basin was relatively large. For example, in Yingxi, Ganchaigou and adjacent regions, huge mixed rock deposits developed in the E_3^2 Member, and the thickest area can be more than two kilometers, meanwhile, this stratigraphic section is also the main source rock development section of western Qaidam basin. It is equivalent to that the source rock has a relatively large burial rate during this period, and the source rock has a relatively fast thermal evolution rate owing to the thick strata of E_3^2 Member. In the Neogene, controlled by the migration of the deposition center, the sedimentary strata gradually became thinner, which is equivalent to the gradually slowing down of the burial rate of the E_3^2 Member source rock and its thermal evolution rate gradually slowing down. The source rocks in this area can reach relatively high maturity in the early burial stage, enter the oil generation window, and form large-scale crude oil, because the Ganchaigou area has this typical "early fast and late slow" thermal evolution characteristics of source rocks.

The formation of the western Qaidam baisn structure was mainly controlled by the reactivation of the ATR and the EKR. The strike-slip fault was greatly affected by the collision of the India-Tibet plate. It began to be active during the deposition of the Lulehe Formation (E_{1+2}) in the Eocene, with an approximate time of 60–45 Ma (Dupont-Nivet et al. 2010; Garzanti and Van Haver 1988; Green et al. 2008; Hu et al. 2015). The activities in this period are mainly characterized by strike-slip, and squeeze escape characteristics in front of Qilian Range (Bush et al. 2016; Cheng et al. 2015; Cheng et al. 2016; Molnar and Tapponnier, 1975), and the formation of a weak extensional environment in western Qaidam basin (Cheng et al. 2018a, b), the tectonic background affected the formation of high-quality source rocks in western Qaidam basin. The tectonic background of the N_1 in the late depositional period was converted into a compression environment (Wu et al. 2021a, b). In the perspective of Wang (2008), the uplifting period of the EKR was from the late Miocene (late deposition of the N_1 Formation) to the early Pliocene (the deposition period of the Xiayoushashan Formation (N_2^1)), and the approximate time was about 15–20 Ma (Wang et al. 2008), the tectonic activities in this period made the deep layer of the western Qaidam basin take shape, with the ability to capture early low-mature oil. From the late Pliocene (deposition period of the Shizigou Formation (N_2^3)) to the Quaternary, the Himalayan orogenic movement intensified, and the uplift of the EKR further intensified (Yin 2008b; Guan et al. 2017), which further expanded the scale of the deep trap of western Qaidam basin. A series of detachment fold structures were formed in the shallow layer, forming a large number of shallow traps. The Himalayan orogenic activity in this period controlled the formation of the main shallow oil reservoirs in the western Qaidam basin.

The evolution process and model of hydrocarbon accumulation in Ganchaigou area have been established. It is believed that the Ganchaigou area mainly experienced two episodes of hydrocarbon charge, the Miocene Shanganchaigou Formation deposition period (~ 27 Ma) and the end of Xiayoushashan Formation deposition period (~ 15 Ma) of Pliocene. Later, it experienced uplifting and destruction after the late Shangyoushashan Formation deposition period, leading to the destruction of the local reservoir (Fig. 11).

During the deposition of the N_1 Member, the traps of the upper member of the Xiaganchaigou Formation of Paleogene began to take shape. Simultaneously, certain predominant reservoirs such as dissolution pores were formed in the

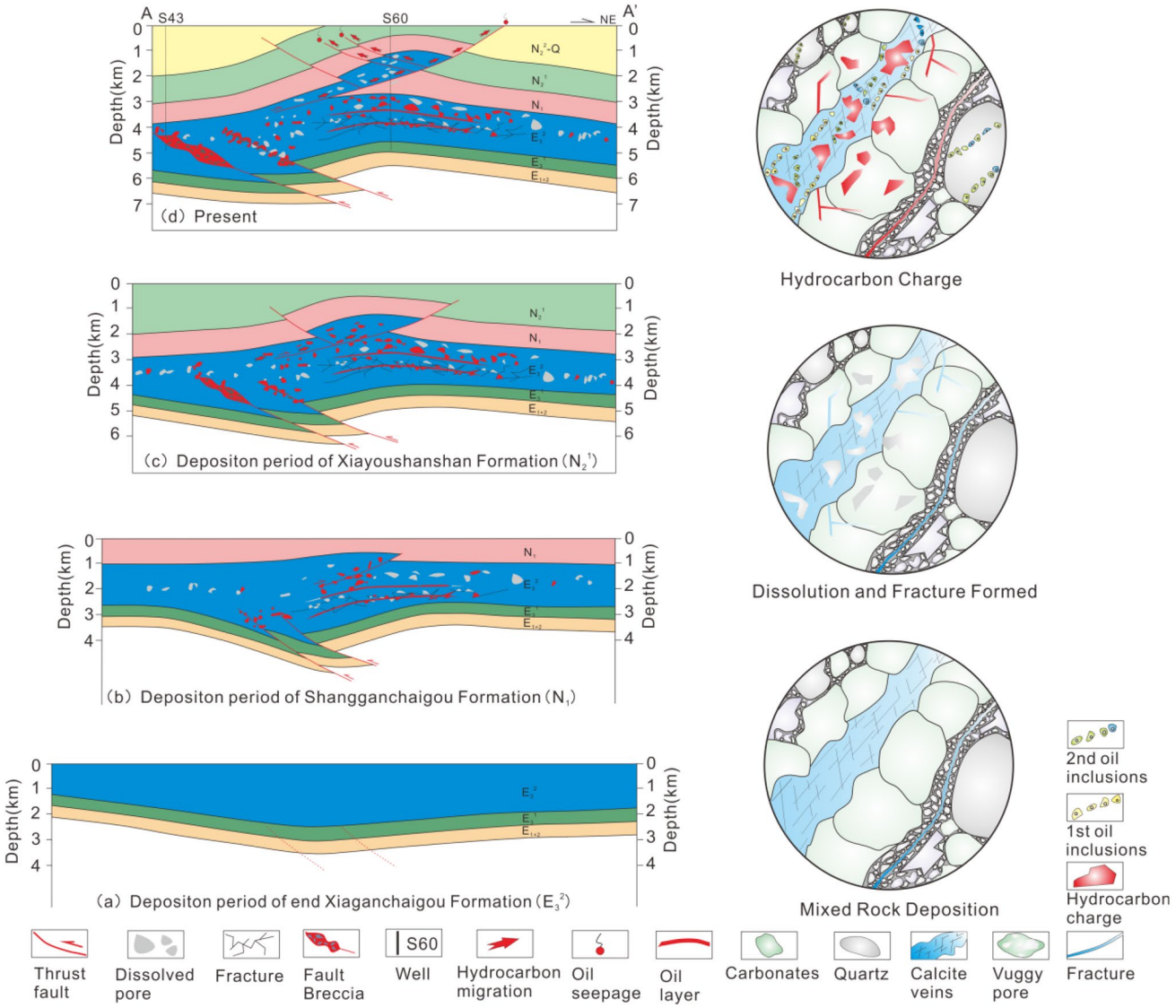

Fig. 11 Schematic diagram of hydrocarbon accumulation process in Ganchaigou area, western Qaidam basin

E_3^2 Member, and early low-mature crude oil was formed and accumulated in low-amplitude traps. In areas such as Ganchaigou and Yingxi, a good salt caprock was deposited in the E_3^2 Member to avoid the loss of early crude oil. At this time, the source rock mainly produces low-mature and some immature crude oil. The presence of a large amount of chloroform bitumen "A" in the low-mature saline lacustrine source rock proves that the source rock has the ability to generate low-mature and immature crude oil (Zhang et al. 2017b). Hydrocarbon charge in this period corresponds to the formation of early low-mature oil inclusions. The fluorescent color is dominated by yellow–brown, and a few yellow-green and blue-green fluorescent inclusions develop. Although the early trap range is low, the dominant mixed rock reservoirs have a wide distribution area, and have the characteristics of self-generation, self-storage and continuous accumulation of shale oil characteristics.

There are three main reasons for the formation of a large-scale hydrocarbon charge in the early stage. (1) The development of saline lacustrine source rocks with specific salinity is conducive to early hydrocarbon generation. Some scholars (Zhang et al. 2017a, 2017b) believe that there are a large number of saline lacustrine source rocks in the western Qaidam basin, and specific algae species (such as coccoliths) can grow in water with certain salinity ranges. The lipid content of algae is particularly high. After being buried and transformed into source rock in the later stage, a large amount of low-mature and immature oil will be generated at the low-mature or immature stage. A large amount of chloroform asphalt "A" is extracted from this kind of low-mature and immature source

rock is the direct evidence of hydrocarbon generation from soluble organic matter (Zhang et al. 2017b). (2) Early rapid stratigraphic burial patterns may also be one of the main reasons for the early rapid maturation of source rocks. When the value of the terrestrial heat flow in a region is constant, the burial rate of the formation plays a key role in the thermal evolution of the source rock. If in the early stage, strata has a fast burial rate and the source rock has a fast early thermal evolution rate, it can reach a higher maturity in the early stage, and in the late stage, strata burial rate is slow, and the source rock thermal evolution rate will be relatively slow. Therefore, Ganchaigou area has a relatively fast burial rate in the early stage, so the source rock can reach the oil generation window in the early stage and generate considerable amount of hydrocarbon, which is recorded by the first stage fluid inclusions. (3) As the E_3^2 Member belongs to a low-porosity and low-permeability reservoir section, the crude oil seepage ability is poor. In addition, due to the stability of the tectonic background in the early period, the hydrocarbon had not experienced the leakage and primary migration, resulting in a large amount of hydrocarbons staying in the reservoir inside the source rock, which is conducive to the formation of a large quantity of early inclusions.

During the depositional period of the Xiayoushashan Formation (N_2^1), tectonic activity furtherly intensified, the amplitude of traps increased, and large-scale shallow traps were formed. Meanwhile, the source rock of the E_3^2 Member is mainly in the peak period of oil generation, and a large amount of mature oil is formed to migrate and accumulate in the shallow strata, forming the characteristics of vertical multilayered hydrocarbon accumulation, corresponding to the formation of blue, blue-white fluorescent mature hydrocarbon inclusions. The intensified tectonic activity has transformed the reservoir of E_3^2 Member, the scale of the dissolution-type cavernous reservoir has increased, and a part of the fractured reservoir has been formed at the same time, which provides favorable conditions for the enrichment of hydrocarbon in the deep strata.

With the deposition of the Shangyoushashan Formation (N_2^2), the Himalayan orogenic movement intensified, leading to the violent uplift of the formation in the Ganchaigou area. A large amount of erosion occurred in the formation, which destroyed the caprock of the shallow strata. The crude oil accumulated in the early shallow strata escaped and dried. The discovery of large-scale oil sands on the surface of Ganchaigou area is the direct evidence of the loss of crude oil during this period. For the deep E_3^2 formation, owing to the sealing of top salt caprock, the deep structural high point is southerly, and the good self-sealing characteristics of the E_3^2 Member, and it has better preservation condition than shallow traps. Therefore, the deep trap of E_3^2 Member of Ganchaigou area still has exploration potential. The discovery of hydrocarbon in part of E_3^2 Member from well S60 is a direct proof, but further work related to the prediction of deep favorable reservoirs or sweet spots is needed.

Conclusions

In the Ganchaigou area, the rock composition of E_3^2 Member is dominated by carbonate rock, and the mineral composition is mainly ankerite. The reservoir space of the mixed rock of E_3^2 Member is dominated by dissolution pores and fractures. The reservoir of E_3^2 Member has obvious characteristics of low porosity and low permeability, and is a typical tight oil reservoir, and the development of fractures in local intervals can increase reservoir permeability.

The Ganchaigou area has experienced two episodes of hydrocarbon charge and the destruction of the shallow reservoirs in the late stage. The first period of hydrocarbon charge was the depositional period of the N_1 Member (about 27 Ma), and the corresponding hydrocarbon inclusions were mainly yellow–brown and yellow fluorescence. The second period of hydrocarbon charge was the deposition period of the N_2^1 Member (about 15 Ma), the fluorescence of the corresponding oil inclusions is mainly blue and blue-white. The QFT analysis results also denote that the composition of current oil reservoirs and palaeo-oil reservoirs are quite different, indicating that it has multiple episodes of oil charge. The late Himalayan orogenic movement destroyed some shallow oil reservoirs, and deep reservoirs still have good prospects for exploration.

The Ganchaigou area experienced charge of low-mature and immature oil during the deposition of the N_1 Member. The source rock burial process, special saline lacustrine source rock development environment and the self-sealing, self-storage characteristics of shale oil led to the accumulation of considerable amount of oil in the E_3^2 Member in early time. At the deposition period of the end of N_2^1 Member, the scale of deep traps expanded, and a series of detachment fold traps formed in shallow layers, accumulated a large amount of mature oil. From the Shangyoushashan Formation to the Quaternary deposition period, the ATR and EKR orogenic activities further intensified, the formation in the Ganchaigou area was violently uplifted, the shallow Neogene oil reservoirs were destroyed, and the deep Paleogene oil reservoirs still have good exploration potential, but further favorable reservoirs selection is needed.

Funding China National Petroleum Corporation Prospective Research Project, Grant No: 2021DJ0303, 2021DJ0302, PetroChina Science and Technology Innovation Project (CN), Grant No: 2016E-0101.

References

Baur F, Hosford Scheirer A, Peters KE (2018) Past, present, and future of basin and petroleum system modeling. AAPG Bull 102(4):549–561. https://doi.org/10.1306/08281717049

Bush MA, Saylor JE, Horton BK, Nie J (2016) Growth of the Qaidam Basin during cenozoic exhumation in the northern Tibetan Plateau: Inferences from depositional patterns and multiproxy detrital provenance signatures. Lithosphere 8(1):58–82. https://doi.org/10.1130/L449.1

Campbell AE (2005) Shelf-geometry response to changes in relative sea level on a mixed carbonate–siliciclastic shelf in the Guyana Basin. Sed Geol 175(1):259–275. https://doi.org/10.1016/j.sedgeo.2004.09.003

Cheng F, Jolivet M, Fu S, Fu S, Zhang Q, Guan S, Yu X, Guo Z (2014) Northward growth of the Qimen Tagh range: a new model accounting for the late Neogene strike-slip deformation of the SW Qaidam Basin. Tectonophysics 632:32–47. https://doi.org/10.1016/j.tecto.2014.05.034

Cheng F, Guo Z, Jenkins HS, Fu S, Cheng X (2015) Initial rupture and displacement on the Altyn Tagh fault, northern Tibetan Plateau: constraints based on residual Mesozoic to Cenozoic strata in the western Qaidam Basin. Geosphere 11(3):921–942. https://doi.org/10.1130/GES01070.1

Cheng F, Jolivet M, Fu S, Zhang C, Zhang Q, Guo Z (2016) Large-scale displacement along the Altyn Tagh Fault (North Tibet) since its Eocene initiation: Insight from detrital zircon U-Pb geochronology and subsurface data. Tectonophysics 677–678:261–279. https://doi.org/10.1016/j.tecto.2016.04.023

Cheng F, Garzione C, Jolivet M, Guo Z, Zhang D, Zhang C (2018a) A new sediment accumulation model of cenozoic depositional ages from the Qaidam basin, Tibetan Plateau. J Geophys Res Earth Surf 123(11):3101–3121. https://doi.org/10.1029/2018JF004645

Cheng X, Zhang D, Jolivet M, Yu X, Du W, Liu R, Guo Z (2018b) Cenozoic structural inversion from transtension to transpression in Yingxiong Range, western Qaidam Basin: new insights into strike-slip superimposition controlled by Altyn Tagh and Eastern Kunlun faults. Tectonophysics 723:229–241. https://doi.org/10.1016/j.tecto.2017.12.019

Cheng F, Garzione CN, Jolivet M, Guo Z, Zhang D, Zhang C, Zhang Q (2019) Initial deformation of the northern Tibetan plateau: insights from deposition of the Lulehe formation in the Qaidam Basin. Tectonics 38(2):741–766. https://doi.org/10.1029/2018TC005214

Chiarella D, Longhitano SG, Tropeano M (2017) Types of mixing and heterogeneities in siliciclastic-carbonate sediments. Mar Pet Geol 88:617–627. https://doi.org/10.1016/j.marpetgeo.2017.09.010

Chung SL, Lo CH, Lee TY (1998) Diachronous uplift of the Tibetan plateau starting 40? Myr Ago. Nat 394(6695):769–773. https://doi.org/10.1038/29511

Dolan JF (1989) Eustatic and tectonic controls on deposition of hybrid siliciclastic/carbonate basinal cycles: discussion with example. AAPG Bull 101(3):422–439. https://doi.org/10.1306/44B4AA0F-170A-11D7-8645000102C1865D

Doyle LJ, Roberts HH (1988) Carbonate-clastic transitions. Elsevier, New York, p p142

Dupont-Nivet G, Lippert PC, Van Hinsbergen DJ, Meijers MJ, Kapp P (2010) Palaeolatitude and age of the Indo-Asia collision: palaeomagnetic constraints. Geophys J Int 182(3):1189–1198. https://doi.org/10.1111/j.1365-246X.2010.04697.x

Feng J, Hu K, Cao J, Wang L (2011) A review on mixed rocks of terrigenous clastic and carbonates and their petroleum-gas geological significance. Geol J China Univ 17(2):297–307

Feng J, Cao J, Hu K, Peng X, Chen Y, Wang Y, Wang M (2013) Dissolution and its impacts on reservoir formation in moderately to deeply buried strata of mixed siliciclastic–carbonate sediments, northwestern Qaidam Basin, northwest China. Mar Pet Geol 39(1):124–137. https://doi.org/10.1016/j.marpetgeo.2012.09.002

Fu B, Awata Y (2007) Displacement and timing of left-lateral faulting in the Kunlun Fault Zone, northern Tibet, inferred from geologic and geomorphic features. J Asian Earth Sci 29(2):253–265. https://doi.org/10.1016/j.jseaes.2006.03.004

Gao G, Yang S, Qu T (2018) Research status of mixing sediments and their relationship with petroleum enrichment. Geol Sci Technol Information 37(06):82–88 (**In Chinese with English abstract**)

García-García F, Soria JM, Viseras C, Fernández J (2009) High-frequency rhythmicity in a mixed siliciclastic–carbonate shelf (Late Miocene, Guadix Basin, Spain): a model of interplay between climatic oscillations, subsidence, and sediment dispersal. J Sediment Res 79(5):302–315. https://doi.org/10.2110/jsr.2009.028

García-Hidalgo JF, Gil J, Segura M, Domínguez C (2007) Internal anatomy of a mixed siliciclastic–carbonate platform: the late cenomanian-mid turonian at the southern margin of the Spanish Central System. Sedimentology 54(6):1245–1271. https://doi.org/10.1111/j.1365-3091.2007.00880.x

Garzanti E, Van Haver T (1988) The indus clastics: Forearc basin sedimentation in the Ladakh Himalaya (India). Sed Geol 59(3–4):237–249. https://doi.org/10.1016/0037-0738(88)90078-4

Goldstein RH (2001) Fluid inclusions in sedimentary and diagenetic systems. Lithos 55(1):159–193. https://doi.org/10.1016/S0024-4937(00)00044-X

Gong L, Fu X, Wang Z, Gao S, Jabbari H, Yue W, Liu B (2019) A new approach for characterization and prediction of natural fracture occurrence in tight oil sandstones with intense anisotropy. AAPG Bull 103(6):1383–1400. https://doi.org/10.1306/12131818054

Gong L, Wang J, Gao S, Fu X, Liu B, Miao F, Zhou X, Meng Q (2021) Characterization, controlling factors and evolution of fracture effectiveness in shale oil reservoirs. J Petrol Sci Eng 203:108655. https://doi.org/10.1016/j.petrol.2021.108655

Green OR, Searle MP, Corfield RI, Corfield RM (2008) Cretaceous-Tertiary carbonate platform evolution and the age of the India-Asia collision along the Ladakh Himalaya (Northwest India). J Geol 116(4):331–353. https://doi.org/10.1086/588831

Guan S, Zhang S, Zhang Y, Yuan X, Guan J, Meng Q, Zhang B (2017) Boundary effect and hydrocarbon accumulation pattern of paleogene hydrocarbon generation depression in the western Qaidam basin. Acta Petrolei Sinica 38(11):1217–1229 (**In Chinese with English abstract**)

Guo R, Zhang Y, Chen X et al (2019) High-frequency cycles and paleogeomorphic characteristics of the upper member of the lower Ganchaigou Formation in Yingxi area Qaidam Basin. Acta Sedimantologica Sinica 37(04):812–824 (**In Chinese with English abstract**)

Gussow WC (1954) Differential entrapment of oil and gas: a fundamental principle. AAPG Bull 38(5):816–853. https://doi.org/10.1306/5CEADF11-16BB-11D7-8645000102C1865D

Harrison TM, Copeland P, Kidd WSF (1992) Raising tibet. Science 255(5052):1663–1670. https://doi.org/10.1126/science.255.5052.1663

Hu X, Garzanti E, Moore T, Raffi I (2015) Direct stratigraphic dating of India-Asia collision onset at the Selandian (middle Paleocene, 59±1 Ma). Geology 43(10):859–862. https://doi.org/10.1130/G36872.1

Jolivet M, Brunel M, Seward D, Xu Z, Yang J, Malavieille J, Wu C (2003) Neogene extension and volcanism in the Kunlun fault zone, northern Tibet: new constraints on the age of the kunlun fault. Tectonics 22(5):1052. https://doi.org/10.1029/2002TC001428

Li ZX, Gao J, Zheng C, Liu CL, Ma YS, Zhao WY (2015) Present-day flow and tectonic –thermal since the late Paleozoic time of the

Qaidam basin. Chin J Geophys 58(10):3687–3705. https://doi.org/10.6038/cjg20151021

Liu K, Eadington P (2005) Quantitative fluorescence techniques for detecting residual oils and reconstructing hydrocarbon charge history. Org Geochem 36(7):1023–1036. https://doi.org/10.1016/j.orggeochem.2005.02.008

Liu K, Eadington P, Middleton H, Fenton S, Cable T (2007) Applying quantitative fluorescence techniques to investigate petroleum charge history of sedimentary basins in Australia and Papuan New Guinea. J Petrol Sci Eng 57(1):139–151. https://doi.org/10.1016/j.petrol.2005.11.019

Liu K, George SC, Lu X, Gong S, Tian H, Gui L (2014) Innovative fluorescence spectroscopic techniques for rapidly characterising oil inclusions. Org Geochem 72:34–45. https://doi.org/10.1016/j.orggeochem.2014.04.010

Liu Z, Zhang Y, Song S, Li S, Long G, Zhao J, Xia Z (2021) Mixed carbonate rocks lithofacies and reservoirs controlling mechanisms in the saline lacustrine basin in Yingxi area, Qaidam Basin NW China. Pet Explor Dev 48(01):80–94. https://doi.org/10.1016/S1876-3804(21)60006-X

Meng QR, Fang X, Burchfiel BC, Wang E (2008) Cenozoic tectonic development of the Qaidam Basin in the northeastern Tibetan Plateau. Investig into Tectonics Tibetan Plateau: Geol Soc Am Special Paper 444:1–24

Meyer B, Tapponnier P, Bourjot L, Metivier F, Gaudemer Y, Peltzer G, Zhitai C (1998) Crustal thickening in Gansu-Qinghai, lithospheric mantle subduction, and oblique, strike-slip controlled growth of the Tibet plateau. Geophys J Int 135(1):1–47. https://doi.org/10.1046/j.1365-246X.1998.00567.x

Molnar P, Tapponnier P (1975) Cenozoic tectonics of Asia: effects of a continental collision. Science 189(4201):419–426. https://doi.org/10.1126/science.189.4201.419

Mount JF (1984) Mixing of siliciclastic and carbonate sediments in shallow shelf environments. Geology 12(7):432–435. https://doi.org/10.1130/0091-7613

Munz IA (2001) Petroleum inclusions in sedimentary basins: systematics, analytical methods and applications. Lithos 55(1):195–212. https://doi.org/10.1016/S0024-4937(00)00045-1

Palermo D, Aigner T, Geluk M, Poeppelreiter M, Pipping K (2008) Reservoir potential of a lacustrine mixed carbonate/siliciclastic gas reservoir: the lower Trassic Rogenstein in the Netherlands. J Pet Geol 31(1):61–96

Ping H, Chen H, Thiéry R, George SC (2017) Effects of oil cracking on fluorescence color, homogenization temperature and trapping pressure reconstruction of oil inclusions from deeply buried reservoirs in the northern Dongying depression, Bohai Bay Basin, China. Mar Pet Geol 80:538–562. https://doi.org/10.1016/j.marpetgeo.2016.12.024

Ping H, Chen H, George SC, Li C, Hu S (2019) Relationship between the fluorescence color of oil inclusions and thermal maturity in the Dongying depression, Bohai Bay Basin, China: Part 1 fluorescence evolution of oil in the context of hydrous pyrolysis experiments with increasing maturity. Mar Pet Geol 100:1–19. https://doi.org/10.1016/j.marpetgeo.2018.10.053

Rashid F, Glover PWJ, Lorinczi P, Collier R, Lawrence J (2015) Porosity and permeability of tight carbonate reservoir rocks in the north of Iraq. J Petrol Sci Eng 133:147–161. https://doi.org/10.1016/j.petrol.2015.05.009

Rashid F, Glover PWJ, Lorinczi P, Hussein D, Lawrence JA (2017) Microstructural controls on reservoir quality in tight oil carbonate reservoir rocks. J Petrol Sci Eng 156:814–826. https://doi.org/10.1016/j.petrol.2017.06.056

Roberts HH (1987) Modern carbonate-siliciclastic transitions: Humid and arid tropical examples. Sed Geol 50(1–3):25–65. https://doi.org/10.1016/0037-0738(87)90027-3

Wang C, Zhao X, Liu Z, Lippert PC, Graham SA, Coe RS, Li Y (2008) Constraints on the early uplift history of the Tibetan Plateau. PNAS 13(105):4987–4992. https://doi.org/10.1073/pnas.0703595105

Wang L (2018) Controlling mechanism of Tertiary saline depositional system on hydrocarbon accumulation of Yingxiongling structural belt in the western Qaidam basin, China. Master's thesis. Research Institute of Petroleum Exploration and Development, Beijing, pp 23–30 **(In Chinese with English abstract)**

Warren JK (2006) Evaporites: sediments, resources and hydrocarbons. Springer Science and Business Media, Berlin

Wu H, Zhao M, Zhuo Q, Lu X (2015) Hydrocarbon accumulation prospect and charge history of the Northern Monocline Belt in Kuqa depression of Tarim basin Western China. Nat Gas Geosci 26(12):2325–2335. https://doi.org/10.1176/j.issn.1672-1926.2015.12.2325 (**In Chinese with English abstract**)

Wu H, Zhao M, Zhuo Q, Xu Z, Bai D, Zhou Y, Zhang B, Wang L (2016a) Hydrocarbon accumulation process analysis of Dina 2 condensate gasfield in Kuqa Depression. J xi'an Shiyou Univ (Nat Sci Edition) 31(03):30–38 (**In Chinese with English abstract**)

Wu H, Zhao M, Zhuo Q, Lu X, Li W, Zeng F, Zhao A (2016b) Palaeofluid evolution process in well block Tubei 1 in the Kuqa depression Tarim Basin. Nat Gas Industry B 3(2):129–138. https://doi.org/10.1016/j.ngib.2016.03.007

Wu H, Zhao M, Zhuo Q, Lu X, Gui L, Li W, Xu Z (2016c) Quantitative analysis of the efect of salt on geothermal temperature and source rock evolution: a case study of Kuqa foreland basin Western China. Pet Explor Dev 43(4):602–610. https://doi.org/10.1016/S1876-3804(16)30070-2

Wu H, Zhao M, Zhuo Q, Lu X, Wang L, Li W, Deng Y (2020) The effect of salt on the evolution of a subsalt sandstone reservoir in the Kuqa foreland basin, western China. Carbonates Evaporites 35(3):1–12. https://doi.org/10.1007/s13146-020-00604-6

Wu H, Zhang Z, Liu S, Wang Z, Zhuo Q, Lu X, Liu H (2021a) Controlling factors of hydrocarbon accumulation and differential distribution in the western Qaidam Basin, Tibet Plateau. Aust J Earth Sci. https://doi.org/10.1080/08120099.2022.2000492

Wu H, Liu S, Wang L, Liu Y, Wang Z, Zhuo Q, Zhang G, Shen X, Liu H (2021b) Fault reactivation and its effect on the formation of source rock——a case study of western Qaidam basin Tibet Plateau. Acta Geologica Sinca 95(06):1921–1934. https://doi.org/10.19762/j.cnki.dizhixuebao.2021b211 (**In Chinese with English abstract**)

Yang C, Sha A (1990) Sedimentary environment of the middle development Qujing formation, Qujing Yunnan Province: a kind of mixing sedimentation of terrigenous clastics and carbonate. Acta Sedimantologica Sinica 02:59–66 (**In Chinese with English abstract**)

Yin A, Dang Y, Zhang M (2007) Cenozoic tectonic evolution of Qaidam Basin and its surrounding regions (part 2): Wedge tectonics in southern Qaidam Basin and the Eastern Kunlun Range. Geol Soc Am Spec Pap 433:369–390. https://doi.org/10.1130/2007.2433(18)

Yin A, Dang YQ, Wang LC, Jiang WM, Zhou SP, Chen XH, McRivette MW (2008a) Cenozoic tectonic evolution of Qaidam basin and its surrounding regions (Part 1): The southern Qilian Shan-Nan Shan thrust belt and northern Qaidam basin. Geol Soc Am Bull 120(7–8):813–846. https://doi.org/10.1130/B26180.1

Yin A, Dang YQ, Zhang M, Chen XH, McRivette MW (2008b) Cenozoic tectonic evolution of the Qaidam basin and its surrounding regions (Part 3): Structural geology, sedimentation, and regional tectonic reconstruction. Geol Soc Am Bull 120(7–8):847–876. https://doi.org/10.1130/B26232.1

Yose LA, Heller PL (1989) Sea-level control of mixed-carbonate-siliciclastic, gravity-flow deposition: lower part of the Keeler Canyon

Formation (Pennsylvanian), southeastern California. GSA Bull 101(3):427–439. https://doi.org/10.1130/0016-7606

Yu J, Pang J, Wang Y, Zheng D, Liu C, Wang W, Xiao L (2019) Mid-Miocene uplift of the northern Qilian Shan as a result of the northward growth of the northern Tibetan Plateau. Geosphere 15(2):423–432. https://doi.org/10.1130/GES01520.1

Zhang L, Ding L, Yang D, Xu Q, Cai F, Liu D (2012) Origin of middle Miocene leucogranites and rhyolites on the Tibetan Plateau: constraints on the timing of crustal thickening and uplift of its northern boundary. Chin Sci Bull 57(5):511–524. https://doi.org/10.1007/s11434-011-4813-4

Zhang B, He Y, Chen Y, Meng Q, Yuan L (2017a) Geochemical characteristics and oil accumulation significance of the high quality saline lacustrine source rocks in the western Qaidam Basin. NW China Acta Petrolei Sinica 38(10):1158–1167 (**In Chinese with English abstract**)

Zhang B, He Y, Chen Y, Meng Q, Huang J, Yuan L (2017b) Formation mechanism of excellent saline lacustrine source rocks in western Qaidam basin. Acta Petrolei Sinica 38(10):1158–1167 (**In Chinese with English abstract**)

Zhao Y, Chen H (2008) The relationship between fluorescence colors of oil inclusions and their maturities. Earth Science J China Univ Geosci 01:91–96 (**In Chinese with English abstract**)

Zhisheng A, Kutzbach JE, Prell WL (2001) Evolution of Asian monsoons and phased uplift of the Himalaya-Tibetan plateau since late miocene times. Nature 411(6833):62. https://doi.org/10.1038/35075035